



## INT Program INT-17-1a

Toward Predictive Theories of Nuclear Reactions Across the Isotopic Chart  
February 27 - March 31, 2017  
and workshop

Nuclear Reactions: A Symbiosis between Experiment, Theory and Applications  
March 13-17, 2017

# Nuclear Exotic Modes and Their Impact on Astrophysical Observables

**Nadia Tsoneva**

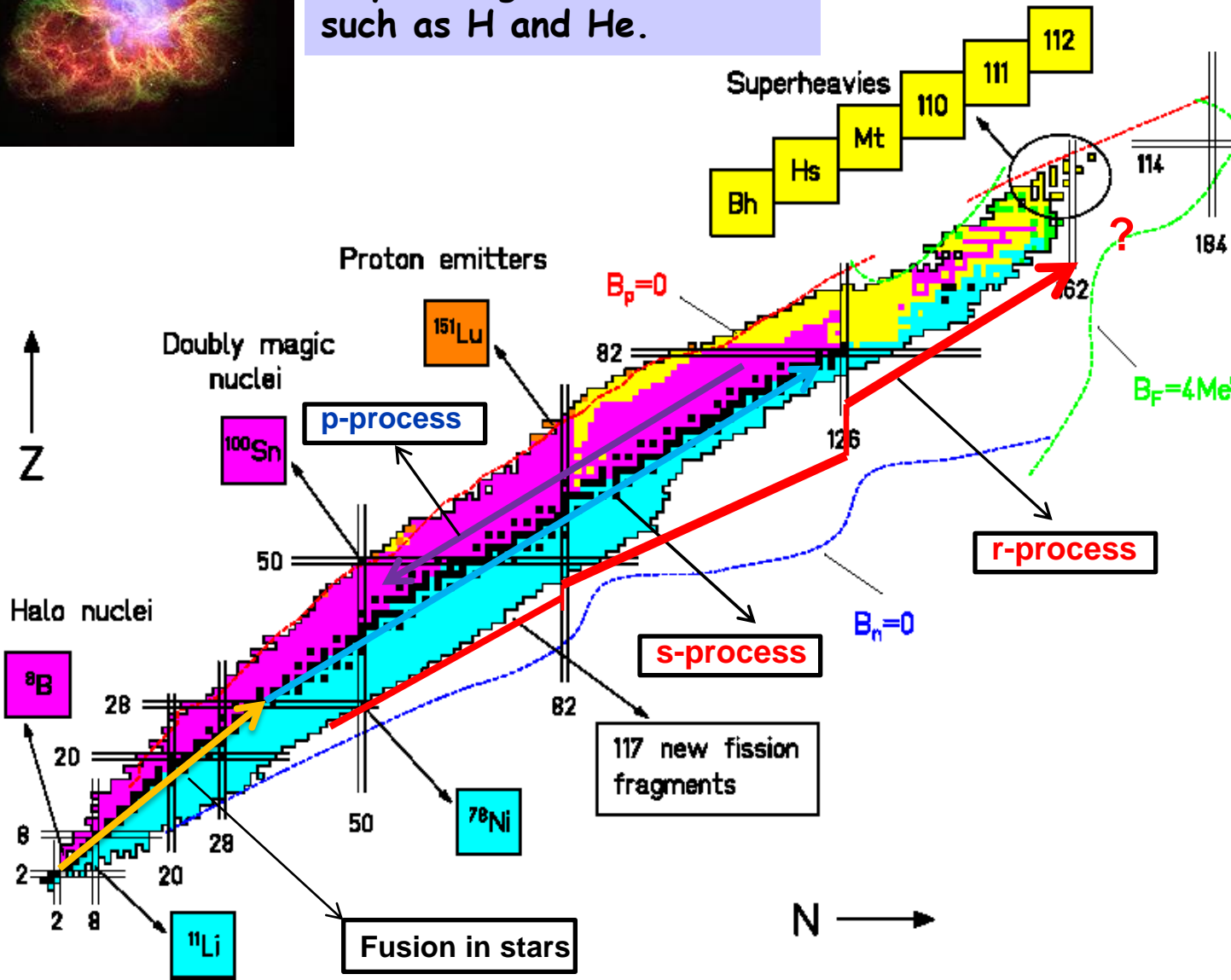
**Institut für Theoretische Physik, Universität Giessen**



# Creation of Elements in Stars



The Big Bang produced only the lightest elements, such as H and He.



How were all the other elements formed?

⇒ nuclear reactions inside stars

"nuclear burning"

⇒ heavier elements,  $Z > 26$  - **n-capture**:

- **s-process** - slow,  $\rho \sim 10^8/\text{cm}^3$ , life time  $\tau \sim 1-10$  years;

- **r-process** - rapid,  $\rho \sim 10^{20}/\text{cm}^3$

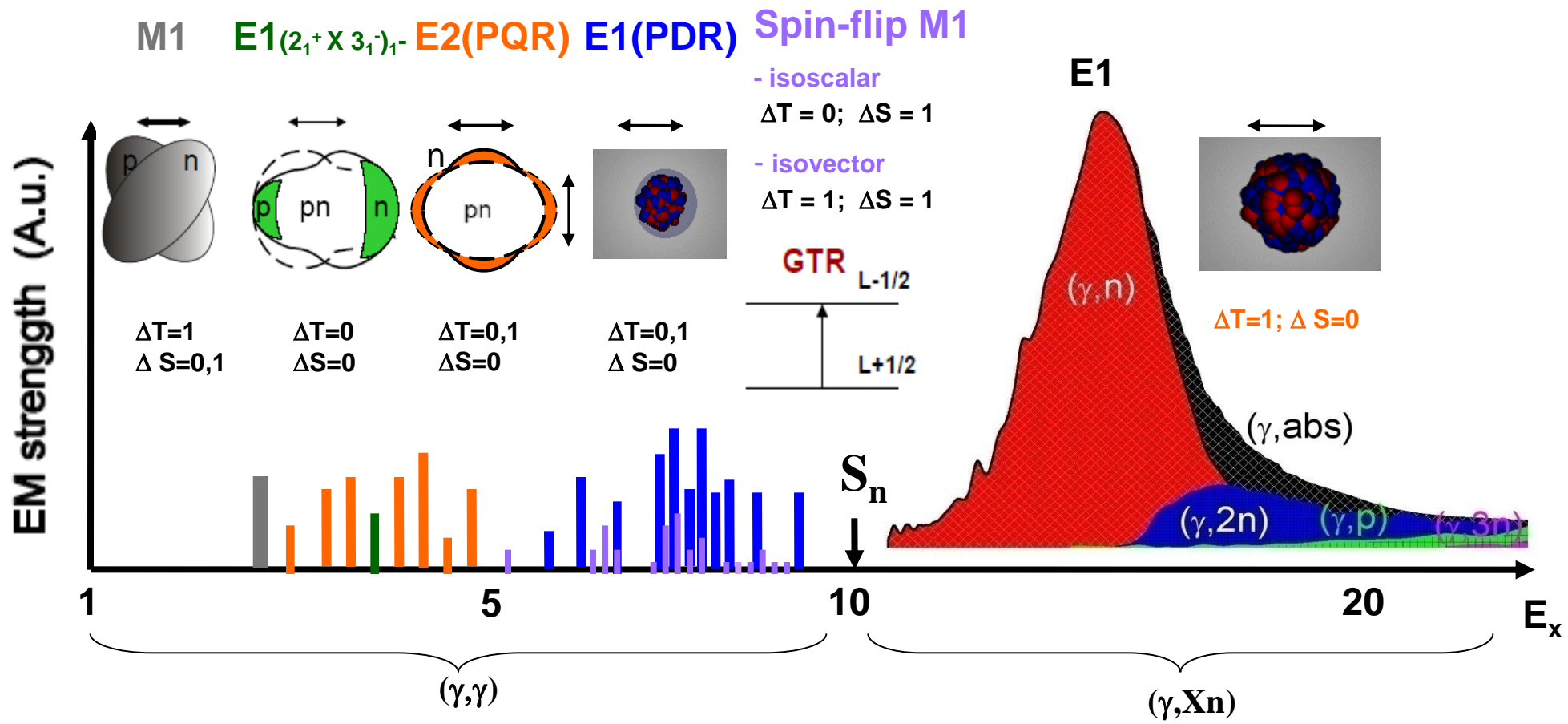
# Agenda

- Pygmy modes: new low-energy modes of excitation in stable and exotic nuclei
- Microscopic theory of low-energy nuclear excitations
- Dipole and quadrupole pygmy modes
- Pygmy modes, dipole polarizability,  $(n,\gamma)$ ,  $(p,\gamma)$  cross sections and nuclear reaction rates of stellar nucleosynthesis.

## Our Goals

- Microscopic approach to infinite matter and finite nuclei
- Ground states and nuclear excitations
- Astrophysical investigations

# The Richness of Nuclear Spectra...



**Moderate and Heavy nuclei :**

- Orbital “Scissors” mode:  $E_x \sim 3$  MeV,  $B(M1) \sim 3 \mu_N^2$
- Two Phonon Excitation:  $E_x \sim 4$  MeV,  $B(E1) \sim 10^{-3}$  W.u.
- Pygmy Quadrupole Resonance:  $E_x \sim 2 - 5$  MeV,  $B(E2) \sim 0.5$  W.u.
- Pygmy Dipole Resonance:  $E_x \sim 6 - 9$  MeV,  $B(E1) \sim 0.5$  W.u.
- Spin-flip M1 excitations:  $E_x \sim 4 - 12$  MeV,  $B(E2) \sim 6 \mu_N^2$
- Giant Dipole Resonance:  $E_x \sim 10 - 20$  MeV,  $B(E1) \sim 5 - 12$  W.u.

Theoretical prediction:  
N. Tsoneva, H. Lenske,  
Phys. Lett. B 695 (2011) 174.



# The Theoretical Model

N. Tsoneva, H. Lenske, Ch. Stoyanov, Phys. Lett. B586, 213 (2004).  
N. Tsoneva, H. Lenske, Phys. Rev. C 77 (2008) 024321.

## The Nuclear Energy-Density Functional: a Functional of Neutron and Proton Densities

$$\mathcal{E}(\rho_n, \rho_p) = \sum_q \tau_q(\rho_q) + \mathcal{E}_{\text{int}}(\rho_n, \rho_p)$$

$\tau_q, \rho_q$  - kinetic and number densities;  $q$  denotes neutrons or protons

$$\mathcal{E}_{\text{int}}(\rho_n, \rho_p) = \mathcal{E}_{\text{int}}(\rho_n^{(0)}, \rho_p^{(0)}) + \sum_q U_q \delta \rho_q + \frac{1}{2} \sum_{q_1, q_2} f_{q_1, q_2} \delta \rho_{q_1} \delta \rho_{q_2}$$

$$U_q = \frac{\delta \mathcal{E}_{\text{int}}}{\delta \rho_q} \quad \text{MF interaction} \longrightarrow$$

Phenomenological GiEDF approach based on a fully microscopic self-consistent Skyrme HFB theory  
F. Hofmann and H. Lenske, Phys. Rev. C57, 2281 (1998).

$$f_{q_1, q_2} = \frac{\delta^2 \mathcal{E}_{\text{int}}}{\delta \rho_{q_1} \delta \rho_{q_2}} \quad \text{residual interaction & nuclear excitations} \longrightarrow$$

Quasiparticle-Phonon Model  
I.V. G. Soloviev: *Theory of Atomic Nuclei: Quasiparticles and Phonons* (Bristol, 1992)./

# The Model Hamiltonian

Quasiparticle-Phonon Model: V. G. Soloviev: Theory of Atomic Nuclei: Quasiparticles and Phonons (Bristol, 1992)

N. Tsoneva, H. Lenske, Ch. Stoyanov, Phys. Lett. B 586 (2004) 213  
N. Tsoneva, H. Lenske, Phys. Rev. C 77 (2008) 024321

$$H = \boxed{H_{MF}} + \boxed{H_{res}}$$

$$H_{MF} = H_{sp} + H_{pair}$$

## Nuclear Ground State

### Single-Particle States

Phenomenological density functional approach based on a fully microscopic self-consistent Skyrme Hartree-Fock-Bogoliubov (HFB) theory

### Pairing and Quasiparticle States

$$a_{jm} = u_j \alpha_{jm} + (-)^{j-m} v_j \alpha_{j-m}^+$$

$$H_{res} = H_M^{ph} + H_{SM}^{ph} + H_M^{pp}$$

### Excited states

$H_M^{ph}$  - multipole interaction in the particle-hole channel;

$H_{SM}^{ph}$  - spin-multipole interaction in the particle-hole channel;

$H_M^{pp}$  - multipole interaction in the particle-particle channel

$$V(|\vec{r} - \vec{r}'|) \approx \sum_{\lambda\mu\tau} (-)^{\mu} R_{\tau}^{\lambda}(r, r') Y_{\lambda\mu}(\theta, \varphi) Y_{\lambda-\mu}(\theta', \varphi')$$

$$R_{\tau}^{\lambda}(r, r') = \kappa_{\tau}^{\lambda} R_{\lambda}(r) R_{\lambda}(r')$$

$\tau = 0$  isoscalar interaction

$\tau = 1$  isovector interaction

# **NUCLEAR EXCITATIONS**

# Theory of Nuclear Excitations

The QPM basis is built of phonons:

$$Q_{\lambda\mu i}^+ = \frac{1}{2} \sum_{\tau} \sum_{jj'}^{n,p} \left\{ \psi_{jj'}^{\lambda i} [\alpha_j^+ \alpha_{j'}^+]_{\lambda\mu} - (-1)^{\lambda-\mu} \varphi_{jj'}^{\lambda i} [\alpha_{j'}^- \alpha_j^-]_{\lambda-\mu} \right\}$$

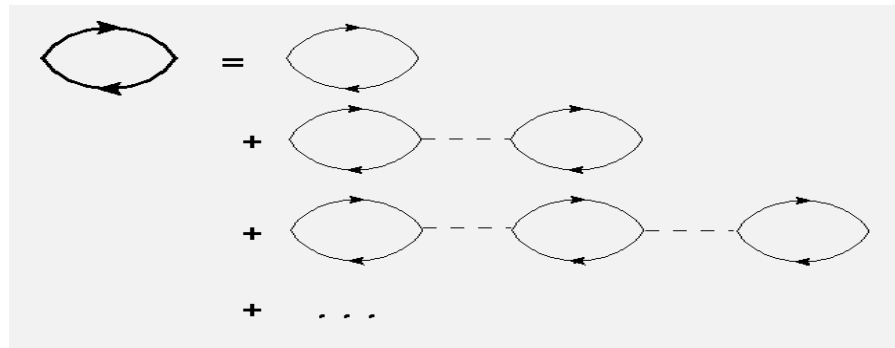
*i* — labels the number of the QRPA state.

The phonons are not 'pure' bosons:

$$[Q_{\lambda\mu i}, Q_{\lambda'\mu'i'}^+] = \delta_{\lambda\lambda'} \delta_{\mu\mu'} \delta_{ii'} + \text{fermionic corrections} \\ \sim \alpha_{j_1 m_1}^+ \alpha_{j_2 m_2}^-$$

QRPA equations are solved:

$$[H, Q_{\lambda\mu i}^+] = E_{\lambda\mu i} Q_{\lambda\mu i}^+$$

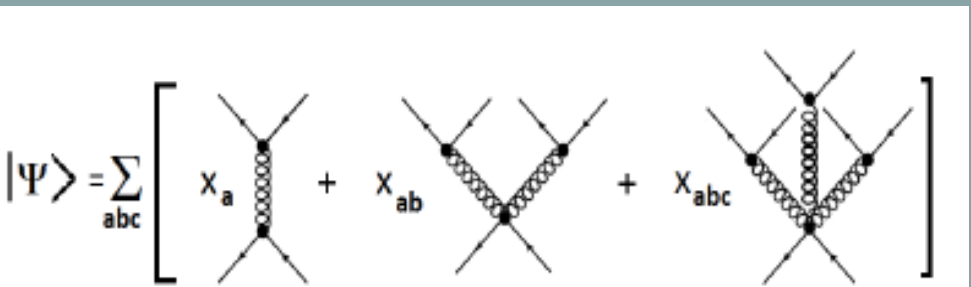


# Beyond QRPA: Including Anharmonicities. Expansions up to 6-QP Components

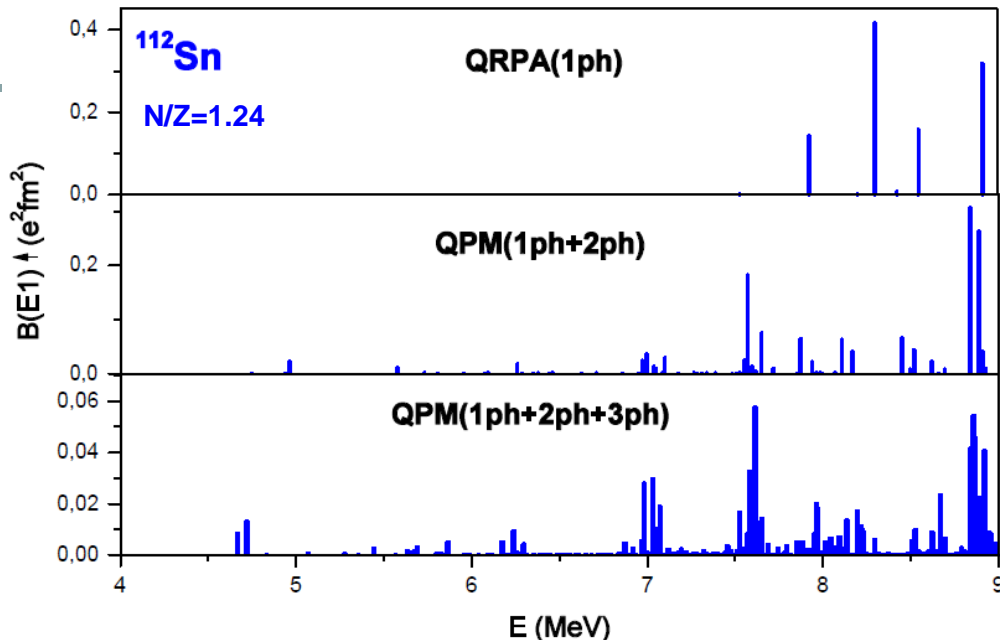
## Multi-Configuration Multi-Quasiparticle Wave Function

$$\Psi_\nu(JM) = \left\{ \sum_i R_i(J\nu) Q_{JMi}^+ + \sum_{\substack{\lambda_1 i_1 \\ \lambda_2 i_2}} P_{\lambda_2 i_2}^{\lambda_1 i_1}(J\nu) [Q_{\lambda_1 \mu_1 i_1}^+ \otimes Q_{\lambda_2 \mu_2 i_2}^+]_{JM} \right. \\ \left. + \sum_{\substack{\lambda_1 i_1 \lambda_2 i_2 \\ \lambda_3 i_3 I}} T_{\lambda_3 i_3}^{\lambda_1 i_1 \lambda_2 i_2 I}(J\nu) [[Q_{\lambda_1 \mu_1 i_1}^+ \otimes Q_{\lambda_2 \mu_2 i_2}^+]_{IK} \otimes Q_{\lambda_3 \mu_3 i_3}^+]_{JM} \right\} \Psi_0$$

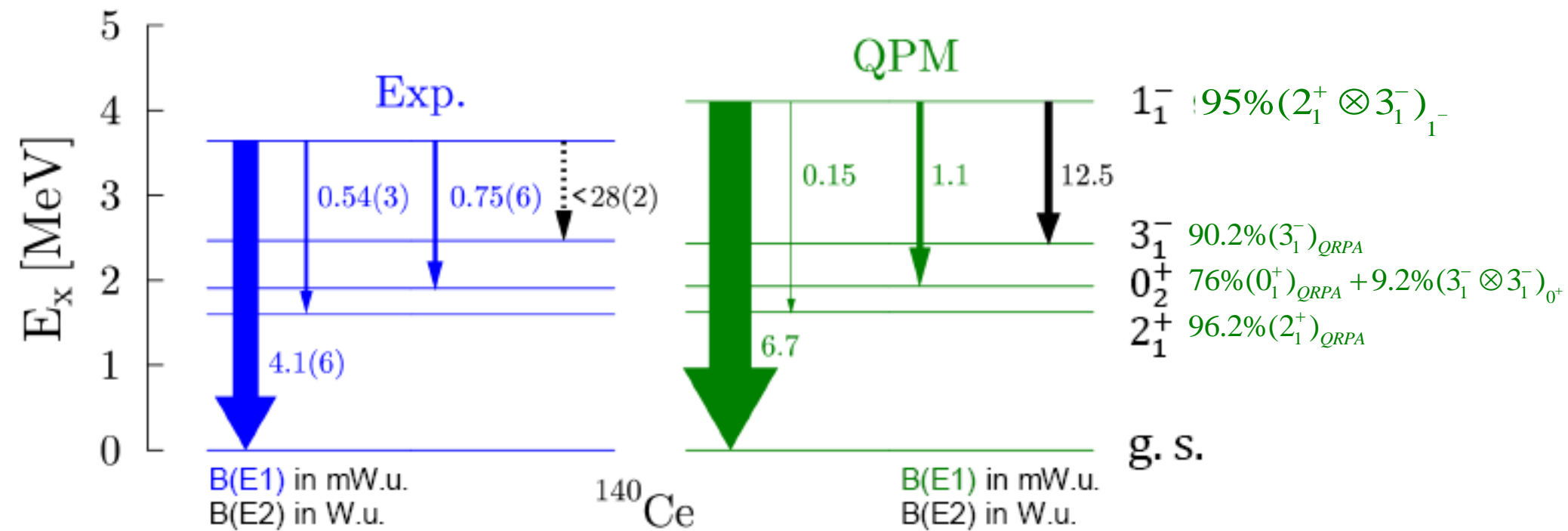
M. Grinberg, Ch. Stoyanov, Nucl. Phys. A. 573 (1994) 231



- Basis of QRPA phonons
- „ph“ and „pp“- type configurations
- Pauli principle, orthogonality
- Core polarization effects
- Large multi-particle-multi-hole configuration space
- **SPECTRAL FRAGMENTATION**
- **SPECTRAL SHIFTS**



# Two-phonon states

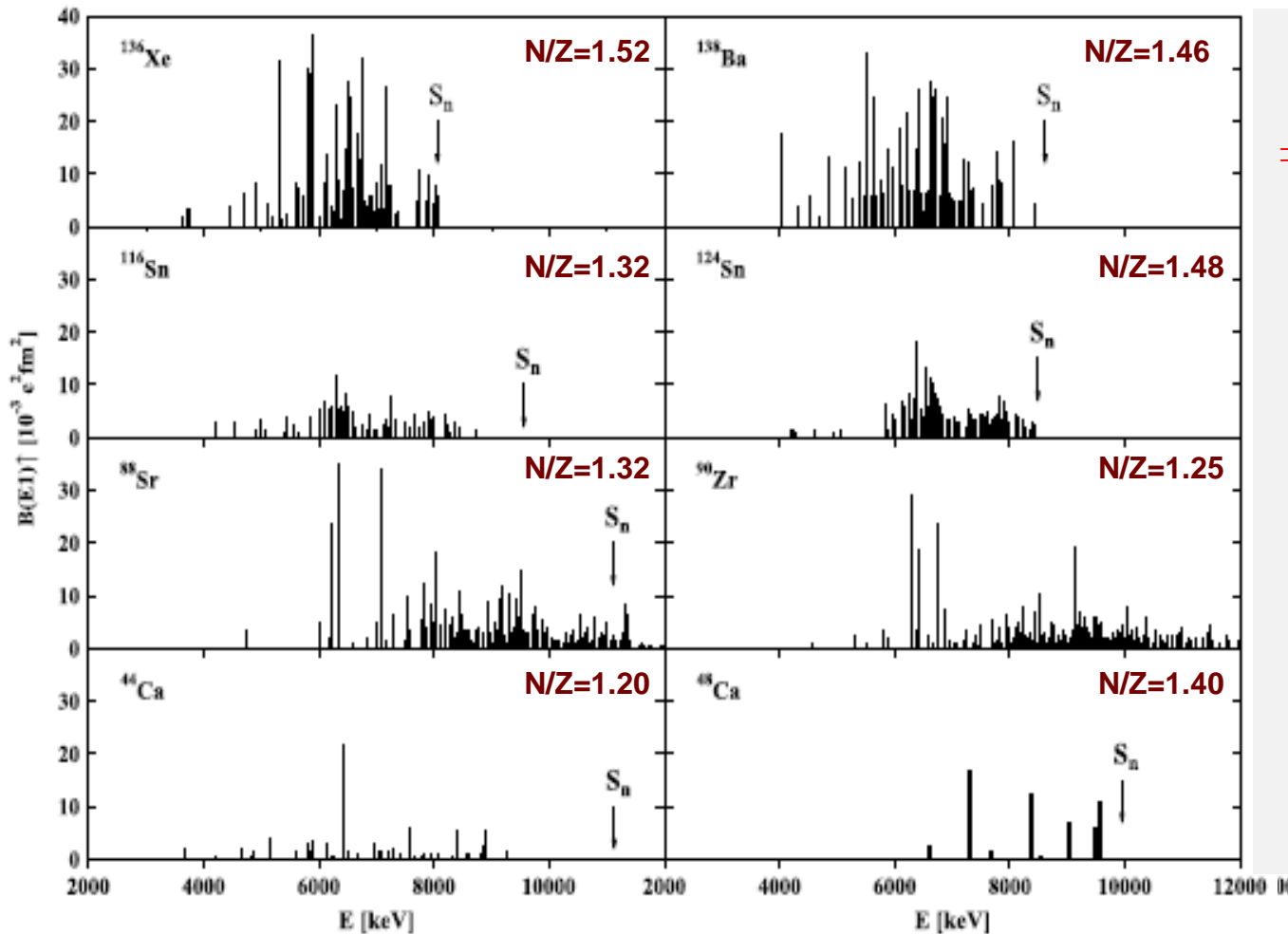


V. Derya, N.Tsoneva, et al., Phys. Rev. C 93, 034311 (2016).

# Observation of Pygmy Dipole Resonance in stable nuclei with moderate neutron excess ( $N > Z$ )

Neutron PDR strength increases with the N/Z ratio !

D. Savran et al. / Progress in Particle and Nuclear Physics 70 (2013) 210–245



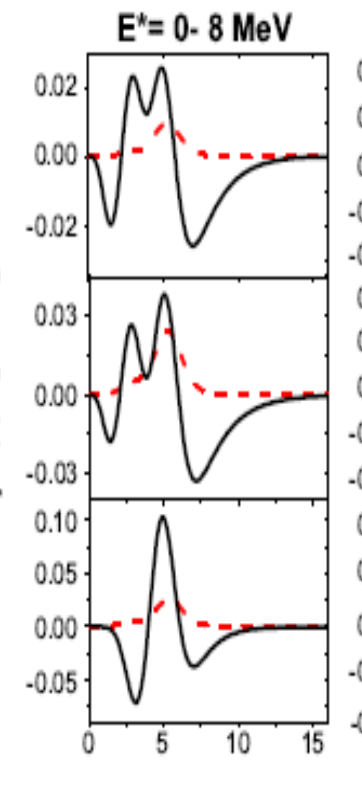
## PDR

- ⇒ Generic mode of excitation;
- ⇒ Below particle threshold;
- ⇒ Independent of the type of nucleon excess
- ⇒ Depending on the size of N/Z;
- ⇒ ~ 1% of the Thomas-Reiche-Kuhn sum rule ( $S_{\text{TRK}} \sim NZ/A$ )

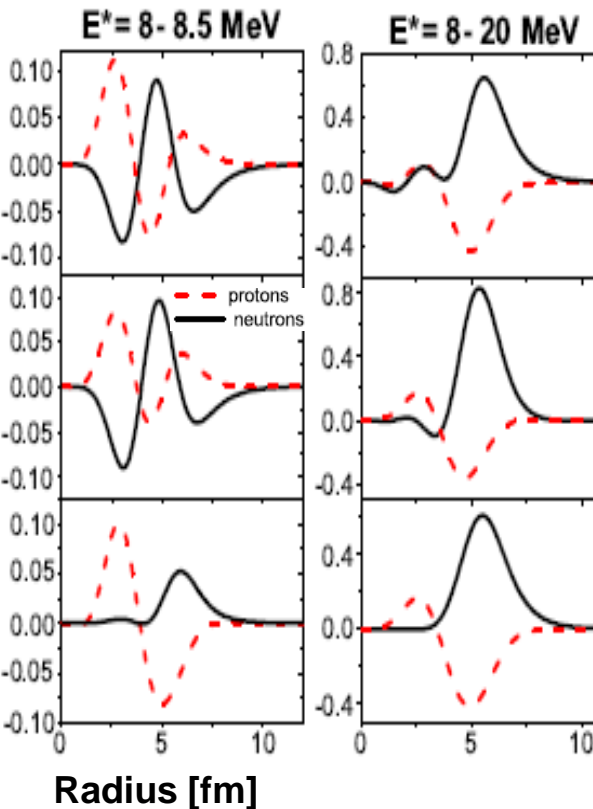
# Identifying the Skin Mode: Dipole Transition Densities in Sn Isotopes

N. Tsoneva, H. Lenske, Ch. Stoyanov, Phys. Lett. B 586 (2004) 213  
 N. Tsoneva, H. Lenske, Phys. Rev. C 77 (2008) 024321

## Neutron PDR

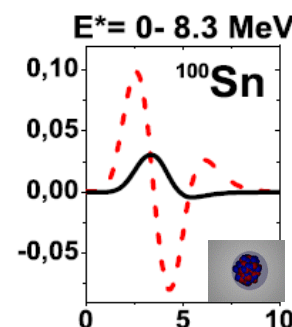


## N>Z

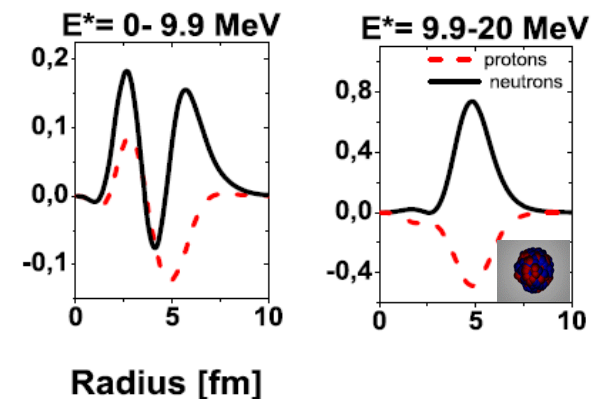


$$\delta\rho^T(\vec{r}) = \sum_{j_1 j_2; \lambda\mu} [i^\lambda Y_{\lambda\mu}(\hat{r})]^\dagger \rho_{j_1 j_2}^{\lambda T}(r) [a_{j_1}^+ a_{j_2}]_{\lambda\mu}$$

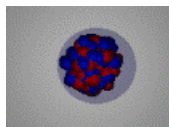
## Proton PDR



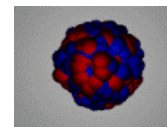
## N=Z



## PDR



## GDR

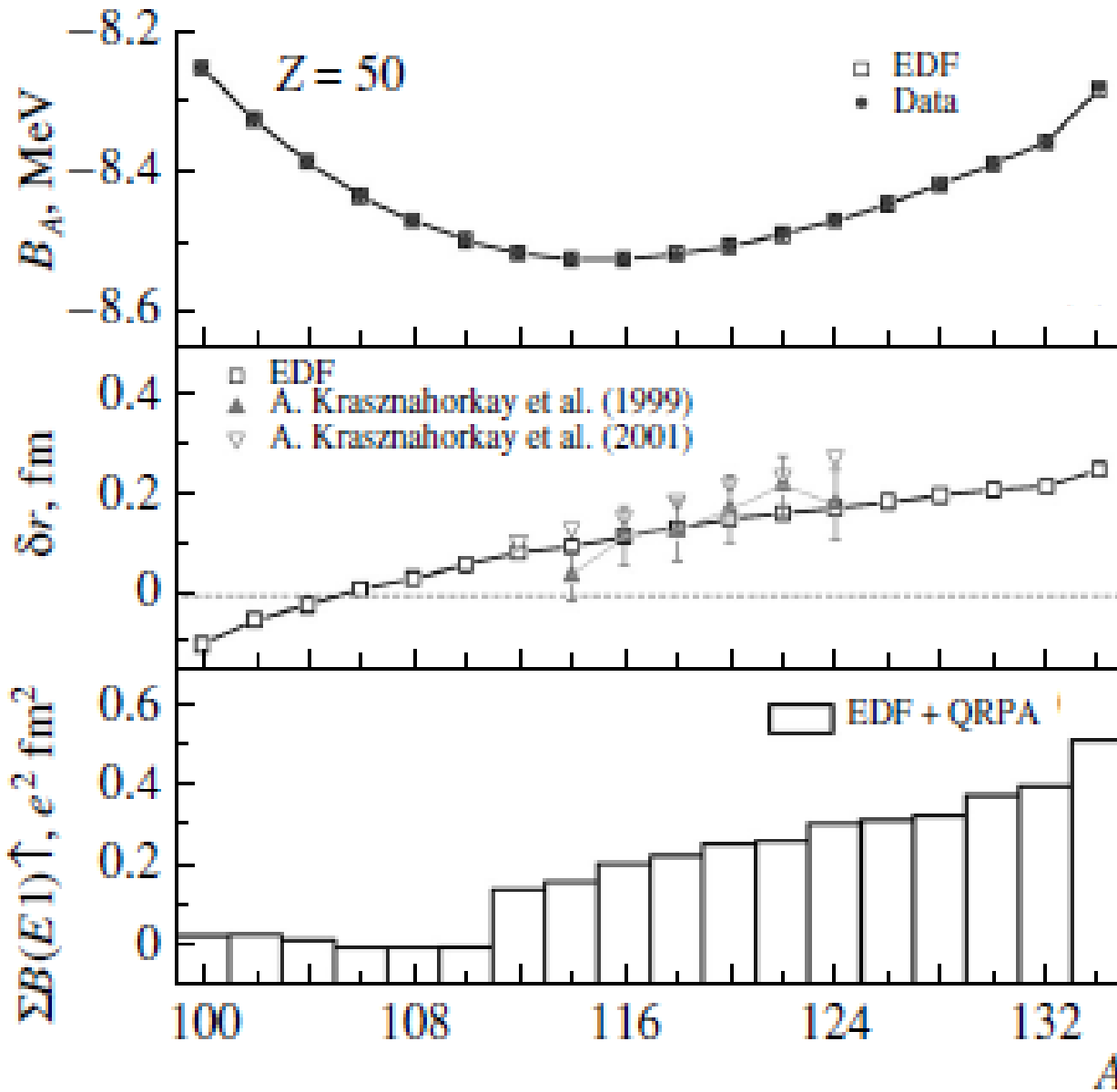


Mixed  
Transient

# Binding Energy, Skin Thickness and PDR

N. Tsoneva, H. Lenske, *Physics of Atomic Nuclei*, 2016, Vol. 76, pp. 885-903.

N. Tsoneva, H. Lenske, PRC 77 (2008) 024321



## Binding Energy

$$B_A(N, Z) = \int d^3r E(\rho_0(r), \rho_1(r)) \\ = \int d^3r (E_{\text{kin}}(r) + E_{\text{int}}(r)).$$

## Skin thickness

$$\delta r = \sqrt{\langle r^2 \rangle_n} - \sqrt{\langle r^2 \rangle_p}$$

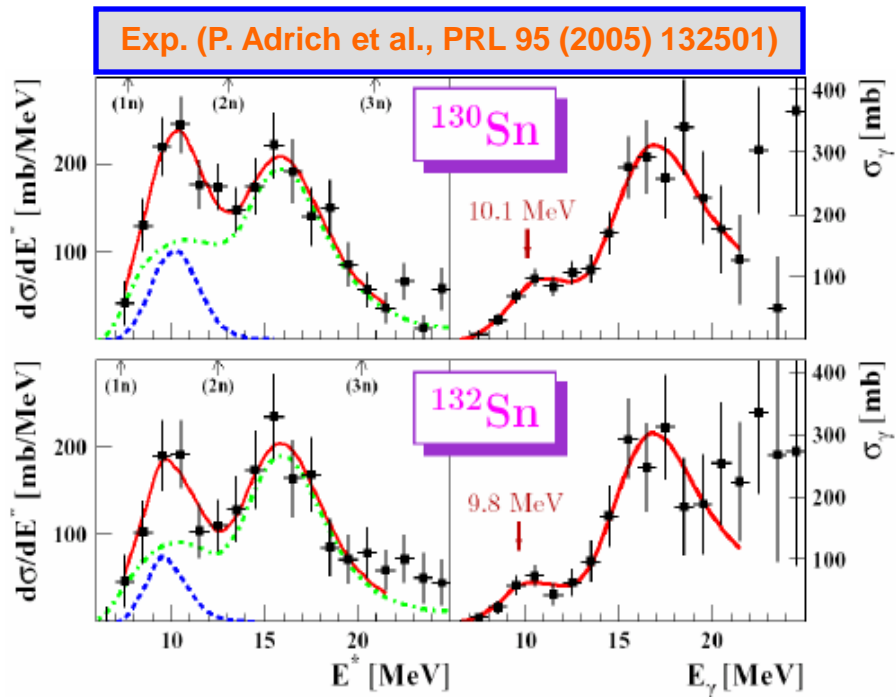
## PDR Strength

$$B(E\lambda) \approx \left[ \sum_{T=1}^1 e_T^\lambda \int_0^\infty r^\lambda \rho_{\lambda i}^T(r) r^2 dr \right]^2$$

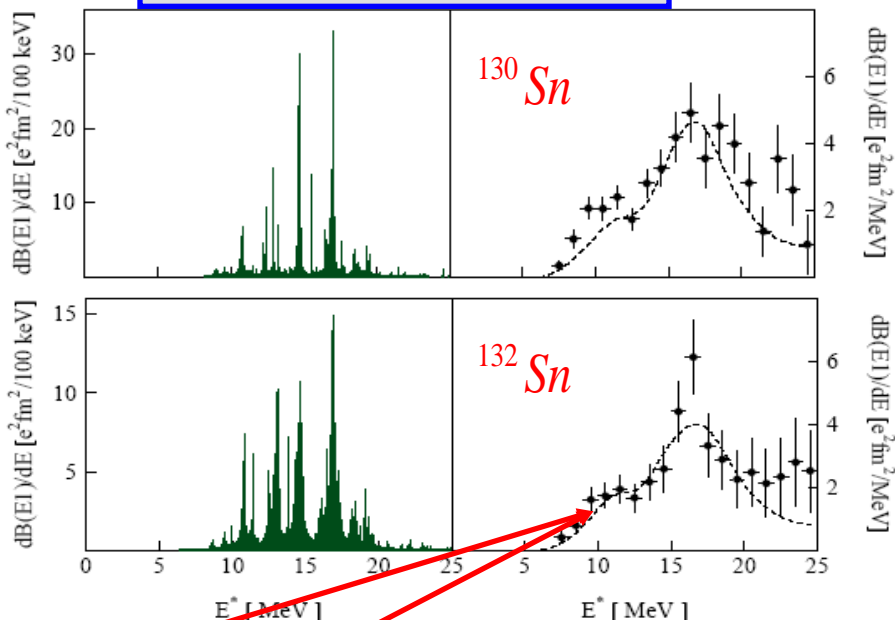
# PDR and GDR states in $^{130,132}\text{Sn}$

In N-rich nuclei: PDR- below the particle threshold, GDR – above the particle threshold

N. Tsoneva, H. Lenske, PRC 77 (2008) 024321



QRPA and LAND-FRS data

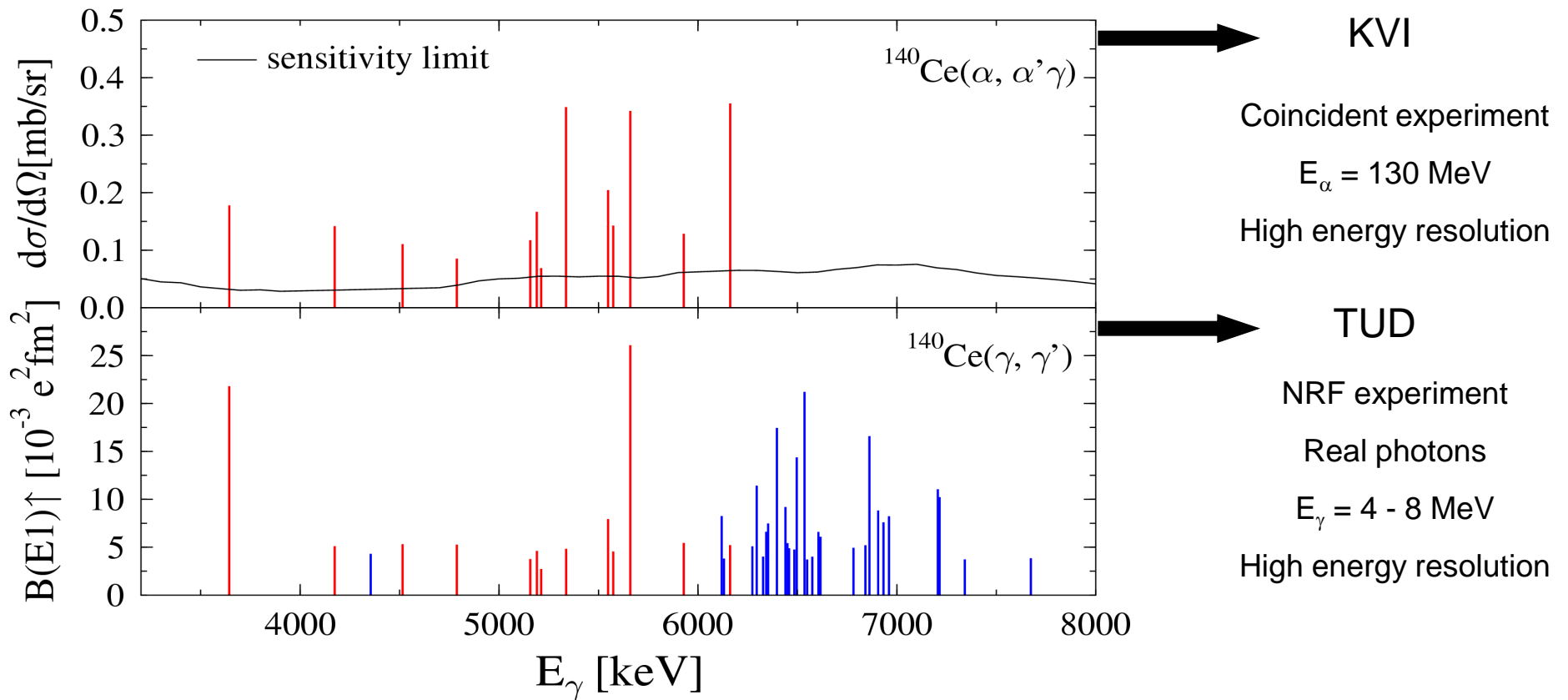


Nucl.	PDR (Energy) [MeV]	$\langle E \rangle_{PDR}$ [MeV]	$\int \sigma^{PDR}$ [mb MeV]	$E_{max}^{PDR}$ [MeV]	$\int \sigma^{PDR}$ [mb MeV]	$E_{LET}^{GDR}$ [MeV]	$\int \sigma^{GDR}$ [mb MeV]	$E_{GDR}^{max}$ [MeV]	$E_{GDR}^{max}$ [MeV]	$\int \sigma^{GDR}$ [mb MeV]	$\int \sigma^{GDR}$ [mb MeV]
	QPM	QPM	QPM	Exp.	Exp.	QPM	QPM	Exp.	QPM	Exp.	QPM
$^{130}\text{Sn}$	0-7.4	5.8	8.2	10.1(7)	130(55)	8-11	137.3	15.9(5)	16.	1930(300)*	1616
$^{132}\text{Sn}$	0-8	7.1	10.4	9.8(7)	75(57)	8-11	97.6	16.1(7)	16.1	1670(420)*	1518

\* The integration is taken up to 20 MeV.

# How to Distinguish the Pygmy Dipole Resonance from Other Modes?

Complementary  $(\alpha, \alpha'\gamma)$  and  $(\gamma, \gamma')$  experiments :  
PDR splits to two parts with different structure



D. Savran et al. PRL, **97** 172505 (2006)

D. Savran et al. NIMA **564** 267 (2006)

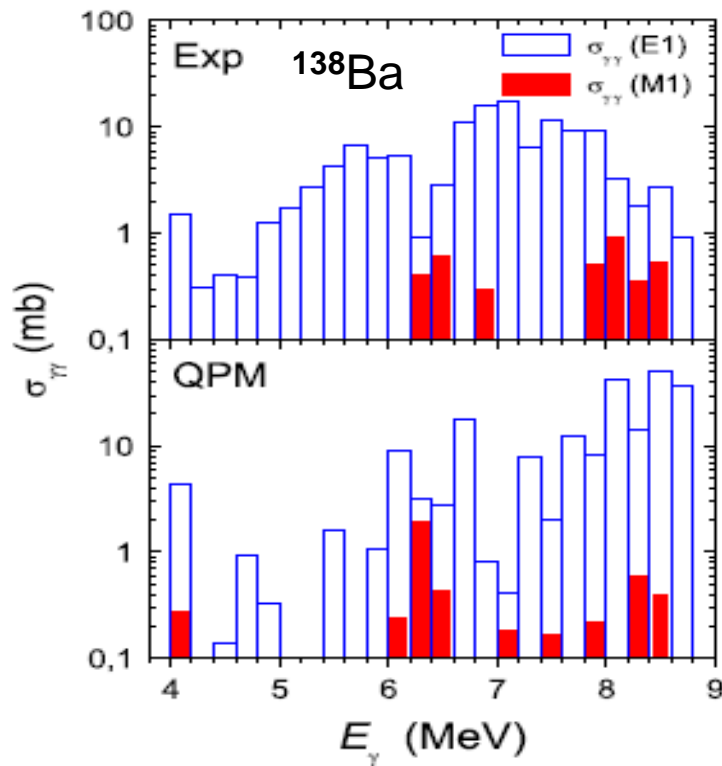
J. Endres et al. PRL **105**, 212503 (2010)

# Parity Measurements of Low-Energy Dipole Excitations in $^{138}\text{Ba}$



First experiment on parity assignment of PDR in  $^{138}\text{Ba}$  at HIγS:  $E_\gamma = 4\text{-}8.5 \text{ MeV}$

A. P. Tonchev, S. L. Hammond, J. H. Kelley, E. Kwan, H. Lenske, G. Rusev, W. Tornow, and N. Tsoneva, Phys. Rev. Lett. 104, 072501 (2010).



$$\sigma_{\gamma\gamma}(M1)/\sigma_{\gamma\gamma}(E1) \sim 3\%$$

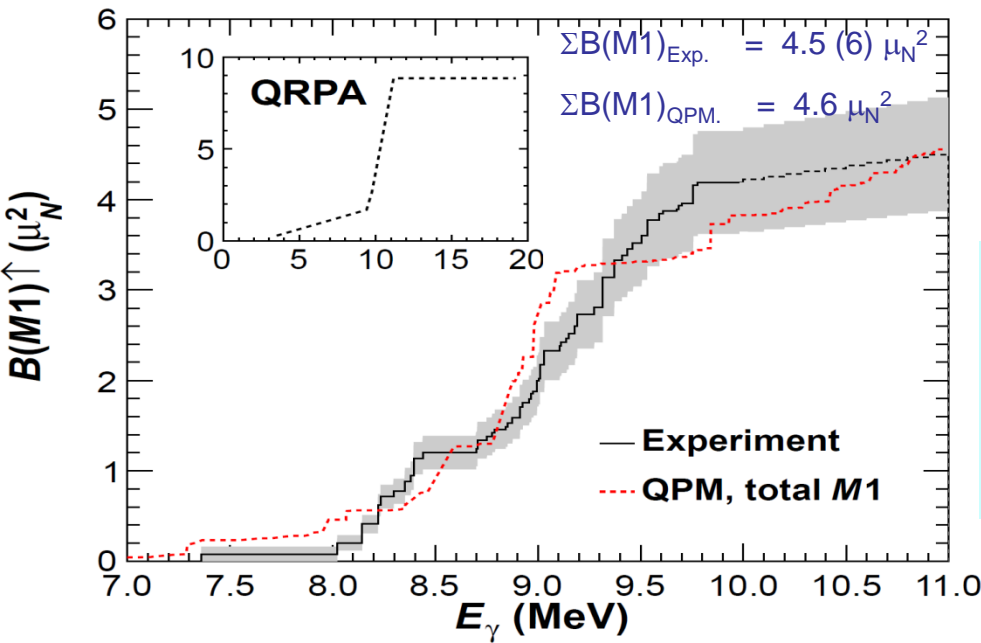
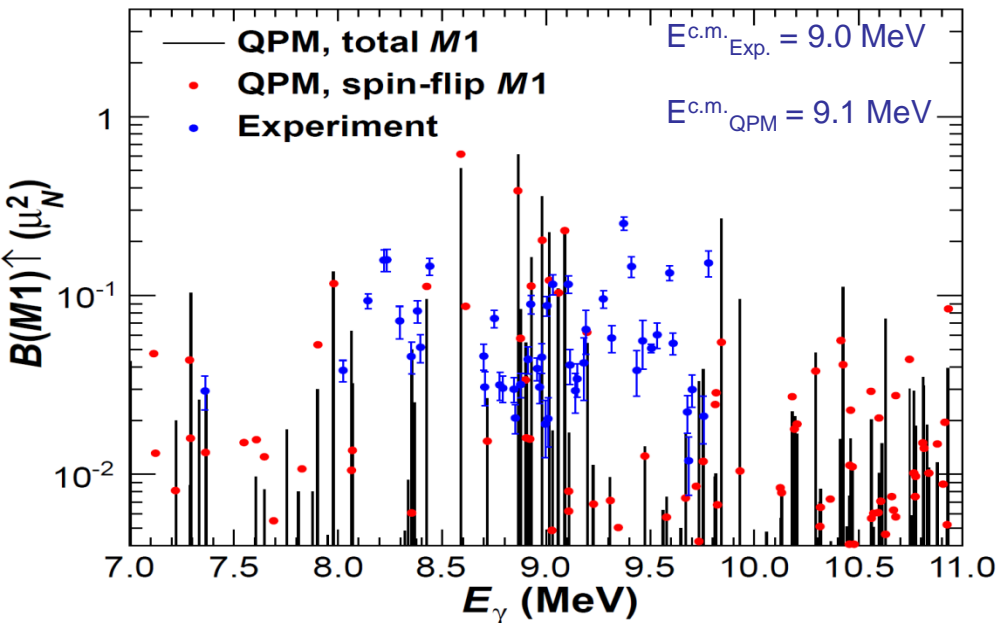
- verified for the first time that the PDR is predominantly E1 in nature.
- The fine structure of the M1 spin-flip mode is explained.
- Low-energy E1 strength fragmentation: Interplay between PDR, multi-phonon excitations and core polarization related to the GDR

TABLE I.  $E1$  and  $M1$  parameters deduced in  $^{138}\text{Ba}$  below the neutron-separation energy in comparison with the QPM calculations.

	$\langle E_{E1} \rangle$ [MeV]	$\Sigma B(E1) \uparrow [e^2 \text{ fm}^2]$	$\langle E_{M1} \rangle$ [MeV]	$\Sigma B(M1) \uparrow [\mu_N^2]$	EWSR $_{E1}$ [%]
Experimental	6.7	0.96(18)	6.9	2.5(6)	1.3
QPM	7.3	1.22	6.9 <sup>a</sup>	2.9 <sup>a</sup>	1.8

<sup>a</sup>4.1 MeV <  $E^*$  < 8.5 MeV.

# Fine Structure Measurements of the Giant M1 Resonance in $^{90}\text{Zr}$ at HI $\gamma$ S



G. Rusev, N. Tsoneva, F. Dönau, S. Frauendorf, R. Schwengner, A. P. Tonchev, A. S. Adekola, S. L. Hammond, J. H. Kelley, E. Kwan, H. Lenske, W. Tornow, and A. Wagner, *Phys. Rev. Lett.* **110**, 022503 (2013).

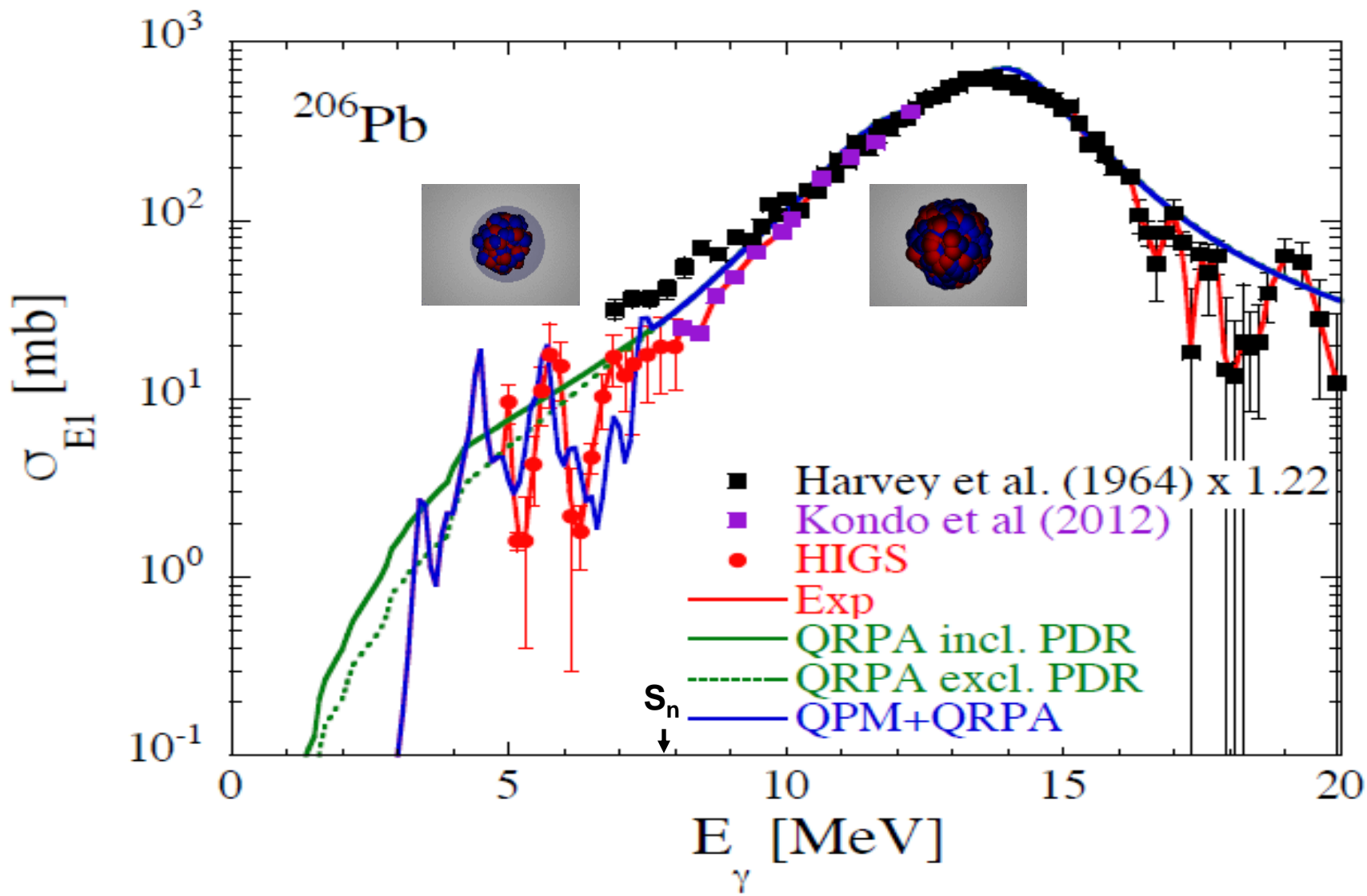
- Explaining the fragmentation pattern and the dynamics of the 'quenching'.
- Multi-particle multi-hole effects increase strongly the orbital part of the magnetic moment.
- QPM prediction of M1 strength at and above the neutron threshold.

Polarized photon scattering off  $^{52}\text{Cr}$ : Determining the parity of  $J=1$  states.

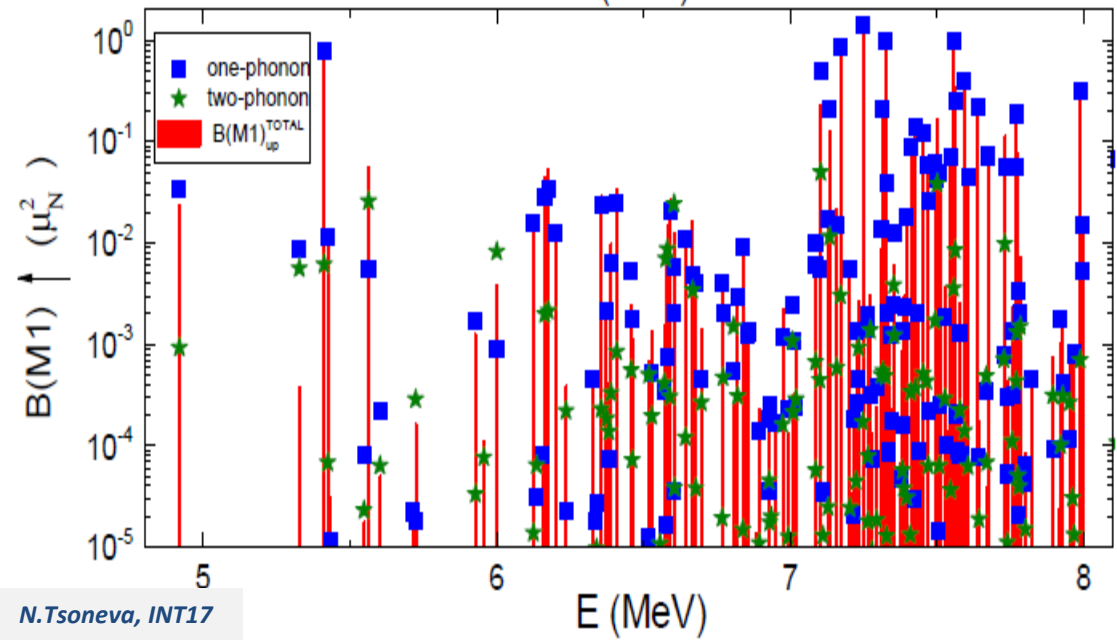
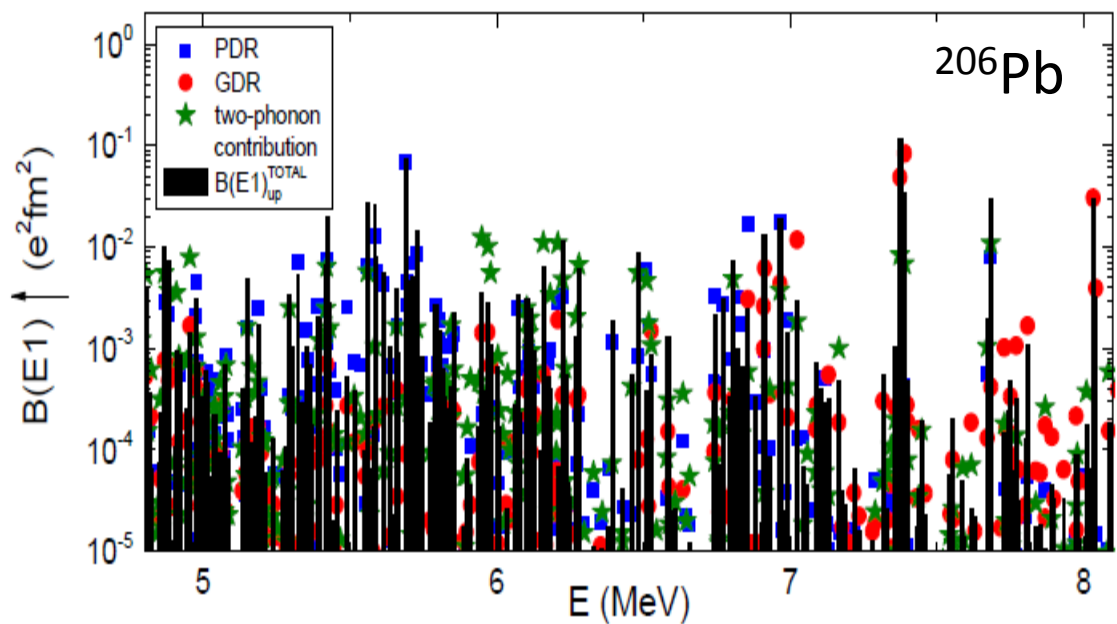
Krishichayan, M. Bhike, W. Tornow, G. Rusev, A. P. Tonchev, N. Tsoneva, and H. Lenske, *PRC* **91**, 044328 (2015).

# Electric Dipole Response in $^{206}\text{Pb}$

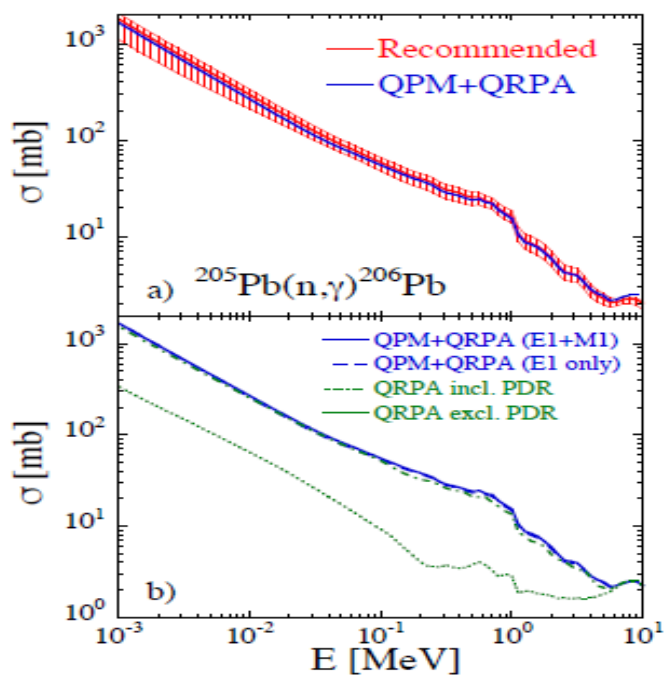
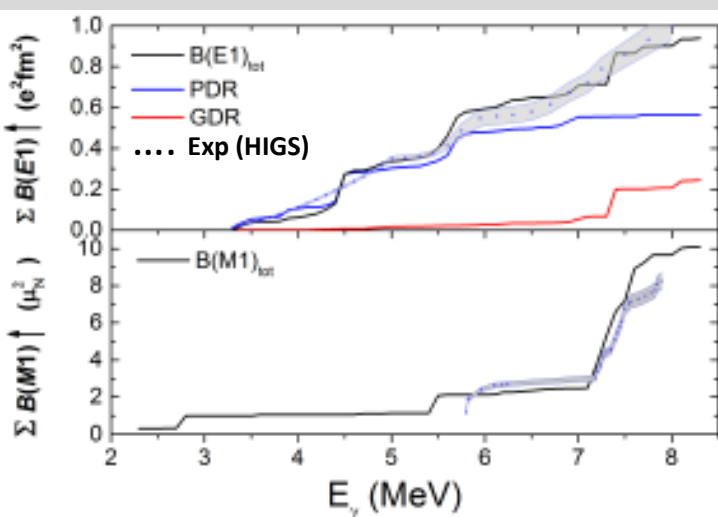
A. Tonchev, N.Tsoneva, S. Goriely, J. Piekarewicz, H. Lenske et al., PRL submitted.



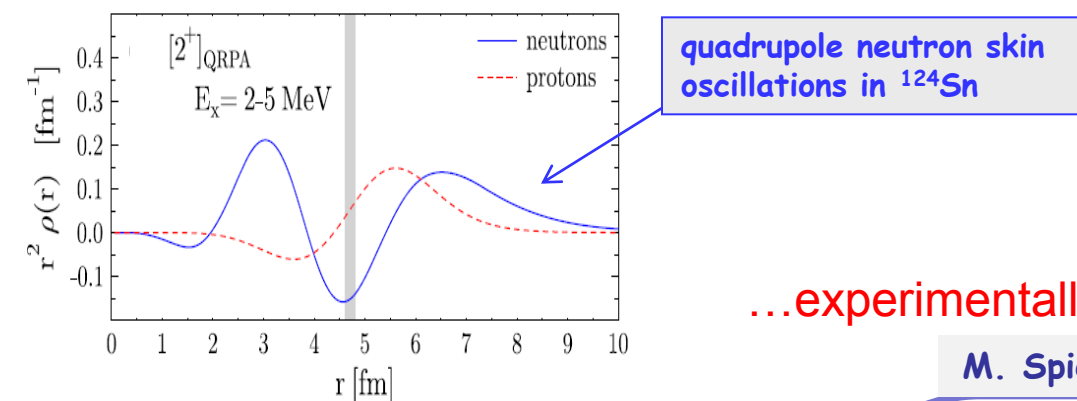
# GiEDF+QPM: Microscopic approach for a unified treatment of multi-phonon excitations, Pygmy- and Giant- Resonances. Astrophysical investigations of $(n,\gamma)$ cross sections.



A. Tonchev, N. Tsoneva, S. Goriely, H. Lenske, J. Piekarewicz, et al., PRL submitted.



# The PQR mode-Quadrupole Oscillations of the Neutron Skin



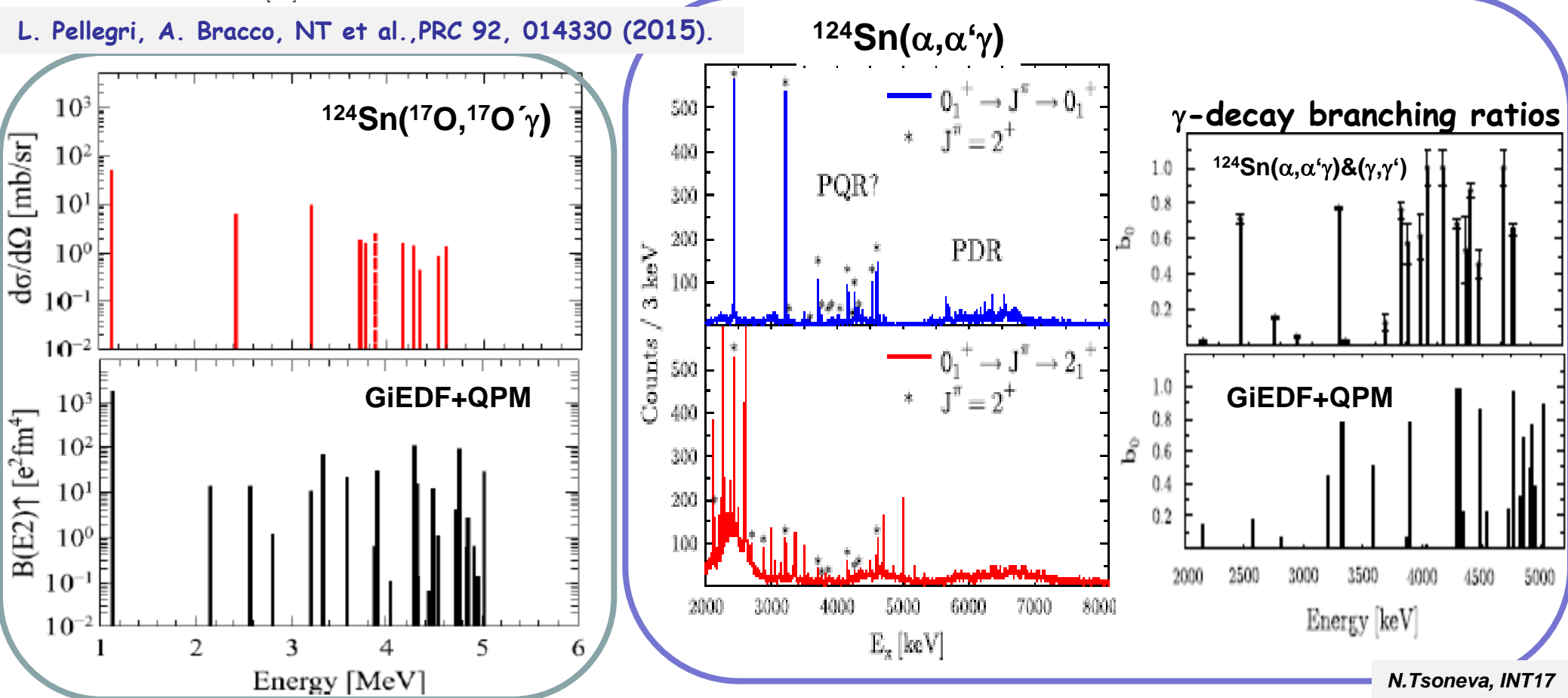
PQR ...theoretically predicted in 2011

N. Tsoneva, H. Lenske, Phys. Lett. B695 174 (2011).

...experimentally confirmed in 2015/2016

M. Spieker, NT et al., Phys. Lett. B752, 102 (2016).

L. Pellegrini, A. Bracco, NT et al., PRC 92, 014330 (2015).

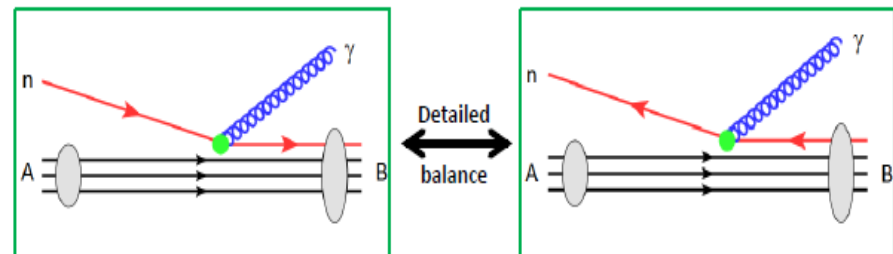


# **NUCLEON CAPTURE CROSS SECTIONS**

# Nuclear Structure and Astrophysical ( $n,\gamma$ ) Capture Cross Sections

- Compound Nucleus Capture: **Hauser-Feshbach Theory** → Statistical Approach at High level densities
- Direct Capture: Population of Identifiable Nuclear States → Microscopic Reaction Theory

- Investigations by Detailed Balance:  $(n,\gamma) \leftrightarrow (\gamma,n)$

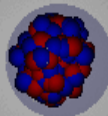


**Total Capture Cross Section: Incoherent Superposition of Electric (E) and Magnetic (M) Multipoles**

$$\sigma(E_{c.m.}) = \sum_{LSJ_i J_f \ell} \frac{8\pi}{2J_f + 1} \frac{\alpha}{v_{\text{rel}}} \frac{q}{1 + q/m_f} \left[ |E_\ell^{LSJ_i J_f}(q)|^2 + |M_\ell^{LSJ_i J_f}(q)|^2 \right]$$

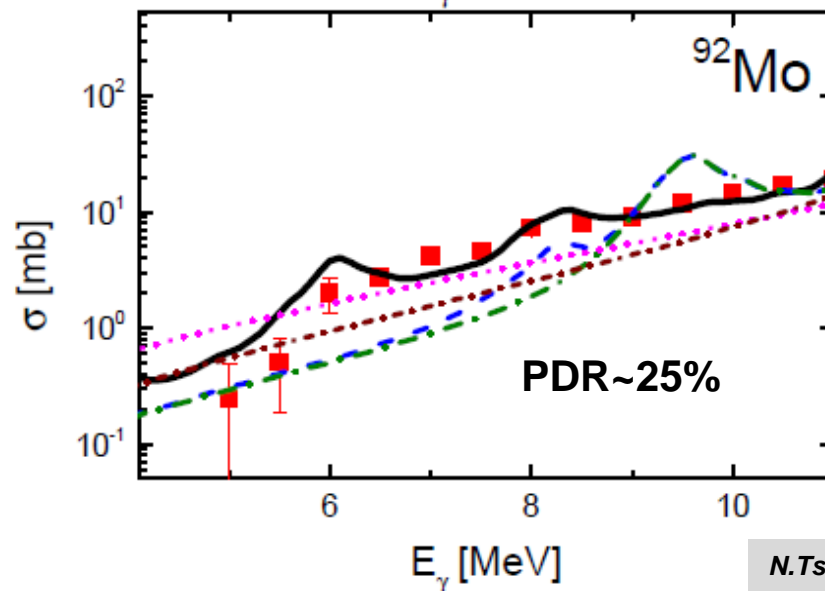
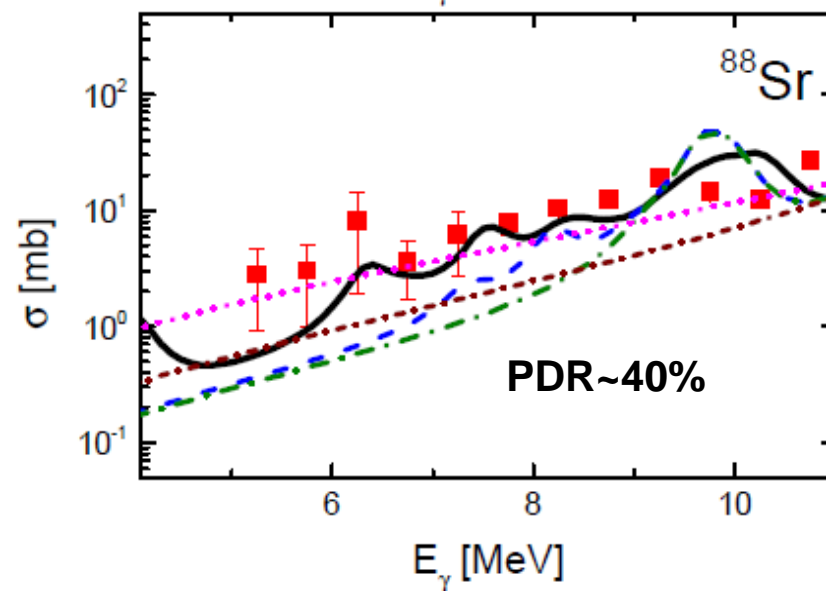
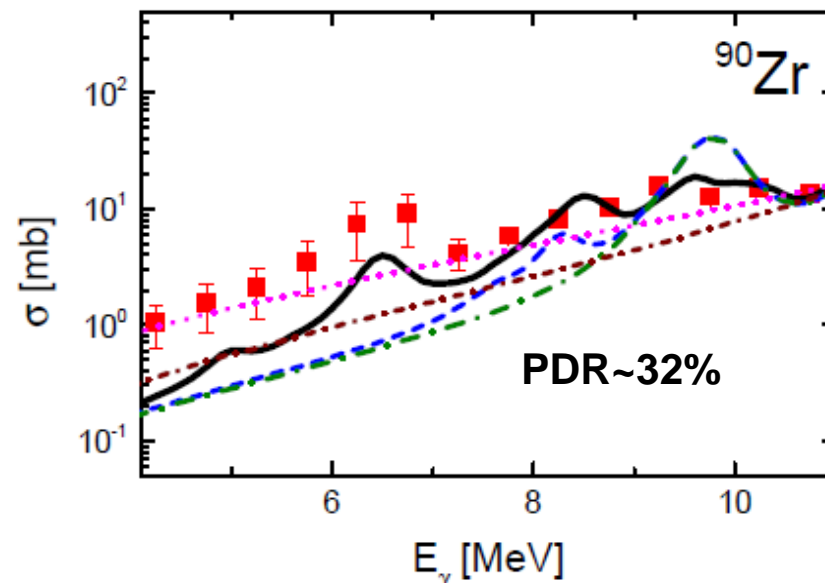
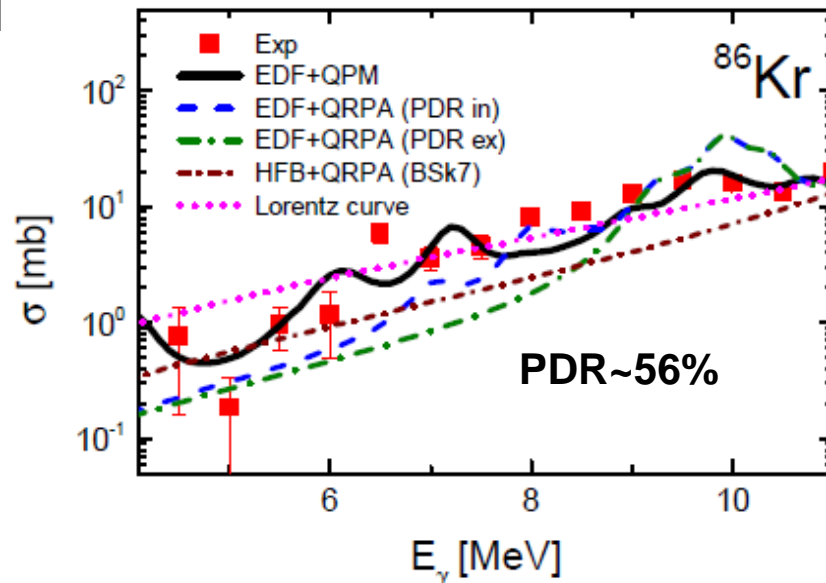
$$E_\ell^{LSJ_i J_f}(q) \xrightarrow[q \rightarrow 0]{(2L+1)!!} \sqrt{B_{J_i J_f}(EL)} \delta_{s0} \text{ etc.}$$

# DYNAMICS OF LOW ENERGY NUCLEAR EXCITATIONS IN N=50 ISOTONES



Exp: R. Schwengner et al., First systematic photon-scattering experiments in N=50 nuclei: using bremsstrahlung produced with electron beams at the linear accelerator ELBE, Rossendorf and quasi-monoenergetic  $\gamma$ -rays at HI $\gamma$ S facility, Duke university.

N. Tsoneva, S. Goriely, H. Lenske, R. Schwengner, Phys. Rev. C91, 044318 (2015).



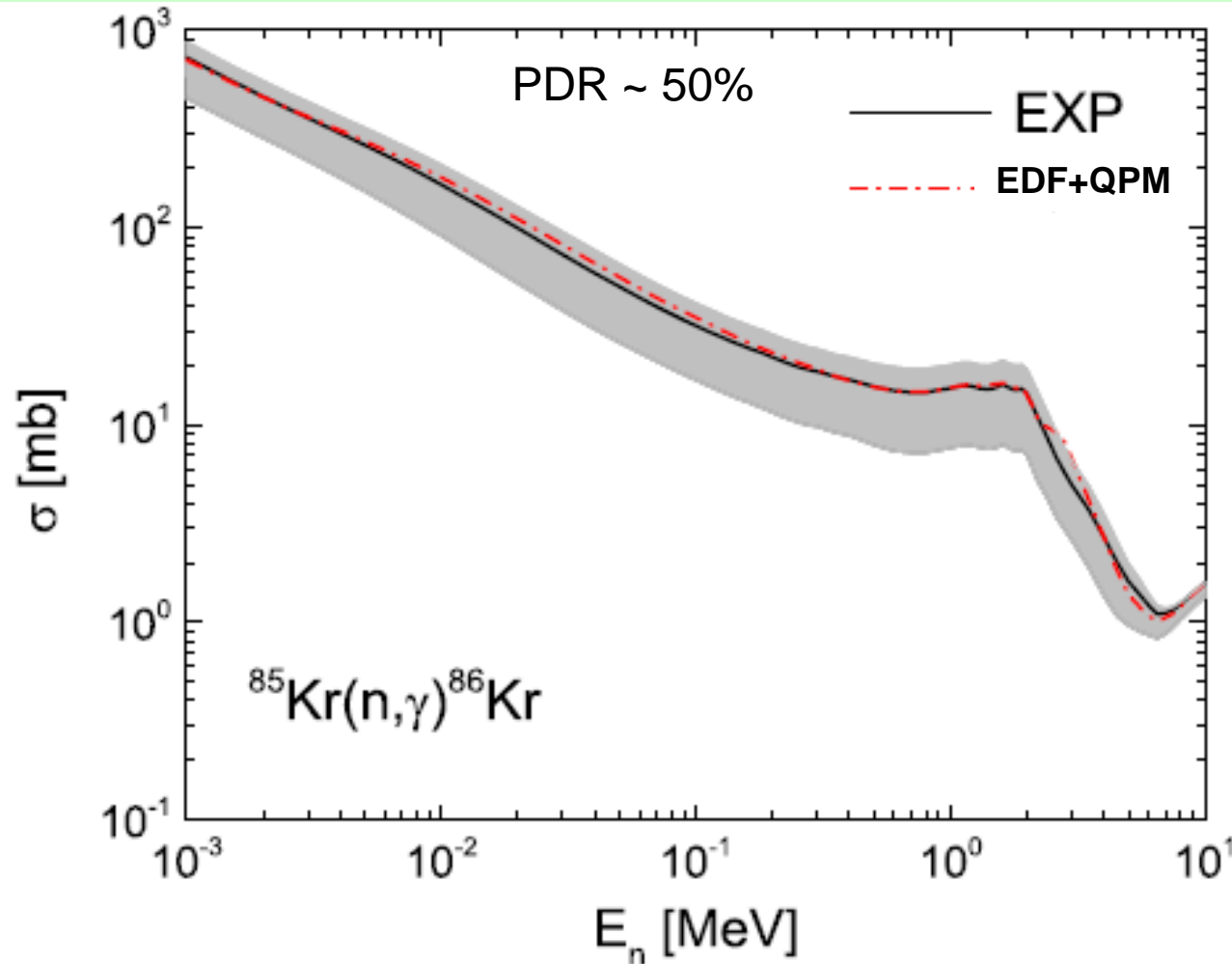
# Total cross section of $^{85}\text{Kr}(n,\gamma)^{86}\text{Kr}$ reaction

R. Raut, A. P. Tonchev, G. Rusev, W. Tornow, C. Iliadis, M. Lugaro, J. Buntain, S. Goriely, J. H. Kelley, R. Schwengner, A. Banu, and N. Tsoneva, Phys. Rev. Lett. 111, 112501 (2013).

N. Tsoneva, S. Goriely, H. Lenske, R. Schwengner, Phys. Rev. C 91, 044318 (2015).

## A way to investigate $^{85}\text{Kr}$ branching point and the s-process:

$^{85}\text{Kr}$  ( $\tau \sim 10.57$  Y) ground state is a branching point and thus a bridge for the production of  $^{86}\text{Kr}$  at low neutron densities.

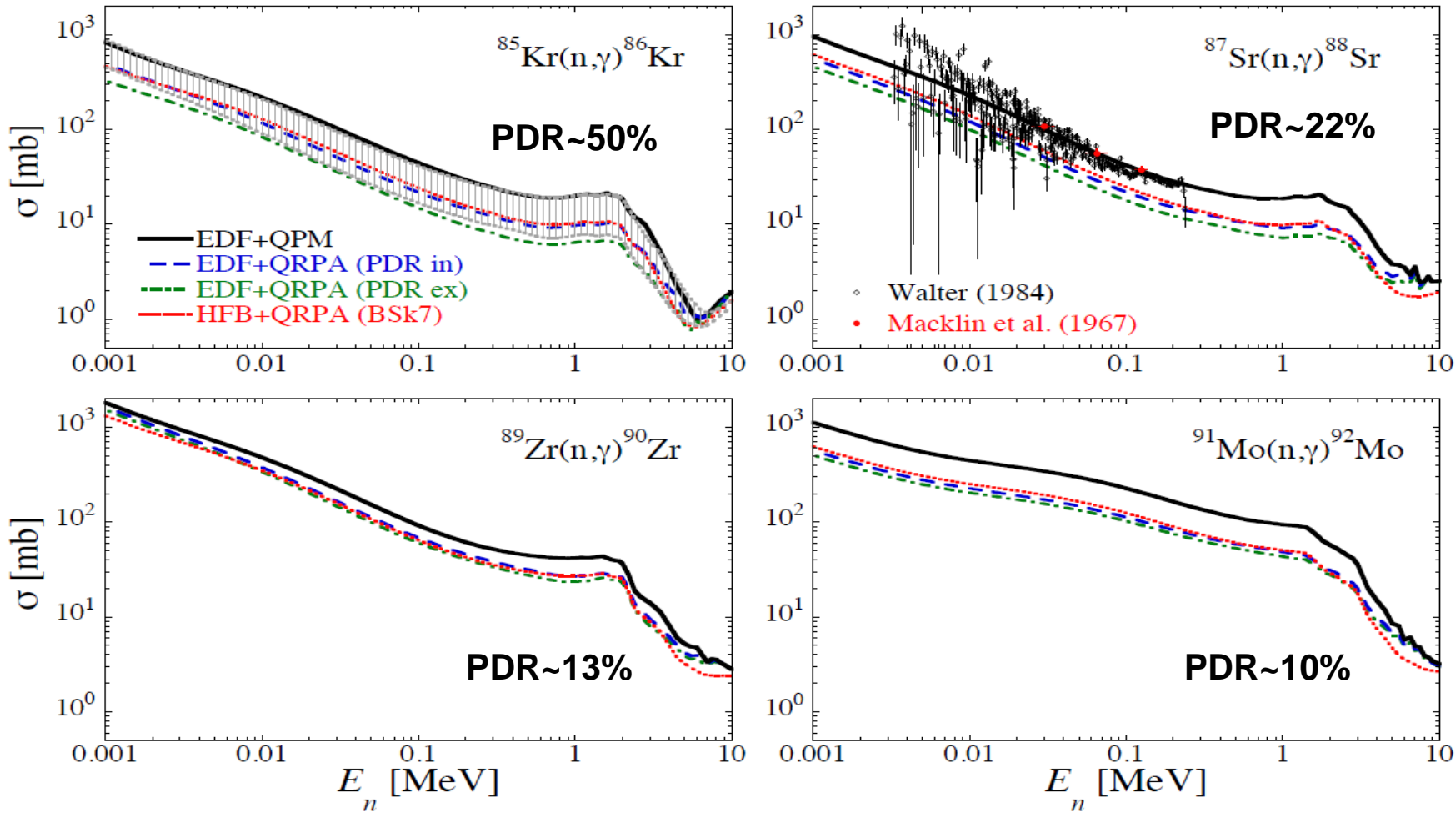


- At stellar temperature of  $kT = 30$  keV we obtain MACS of  $83(+23,-38)$  mb which is about 50% higher than the value of Z.Y. Bao *et al.*, At. Data Nucl. Data Tables 76, 70 (2000).
- The new MACS value explains the higher  $^{86}\text{Kr}:^{82}\text{Kr}$  ratios measured in large star dust SiC grains.
- The experimental uncertainty is improved by a factor of  $\sim 3$  to 50%.

# NEUTRON CAPTURE CROSS SECTIONS

of the  $^{85}\text{Kr}(n,\gamma)^{86}\text{Kr}$ ,  $^{87}\text{Sr}(n,\gamma)^{88}\text{Sr}$ ,  $^{89}\text{Zr}(n,\gamma)^{90}\text{Zr}$  and  $^{91}\text{Mo}(n,\gamma)^{92}\text{Mo}$  reactions calculated with TALYS  
using EDF+QRPA, HFB+QRPA and EDF+three-phonon QPM

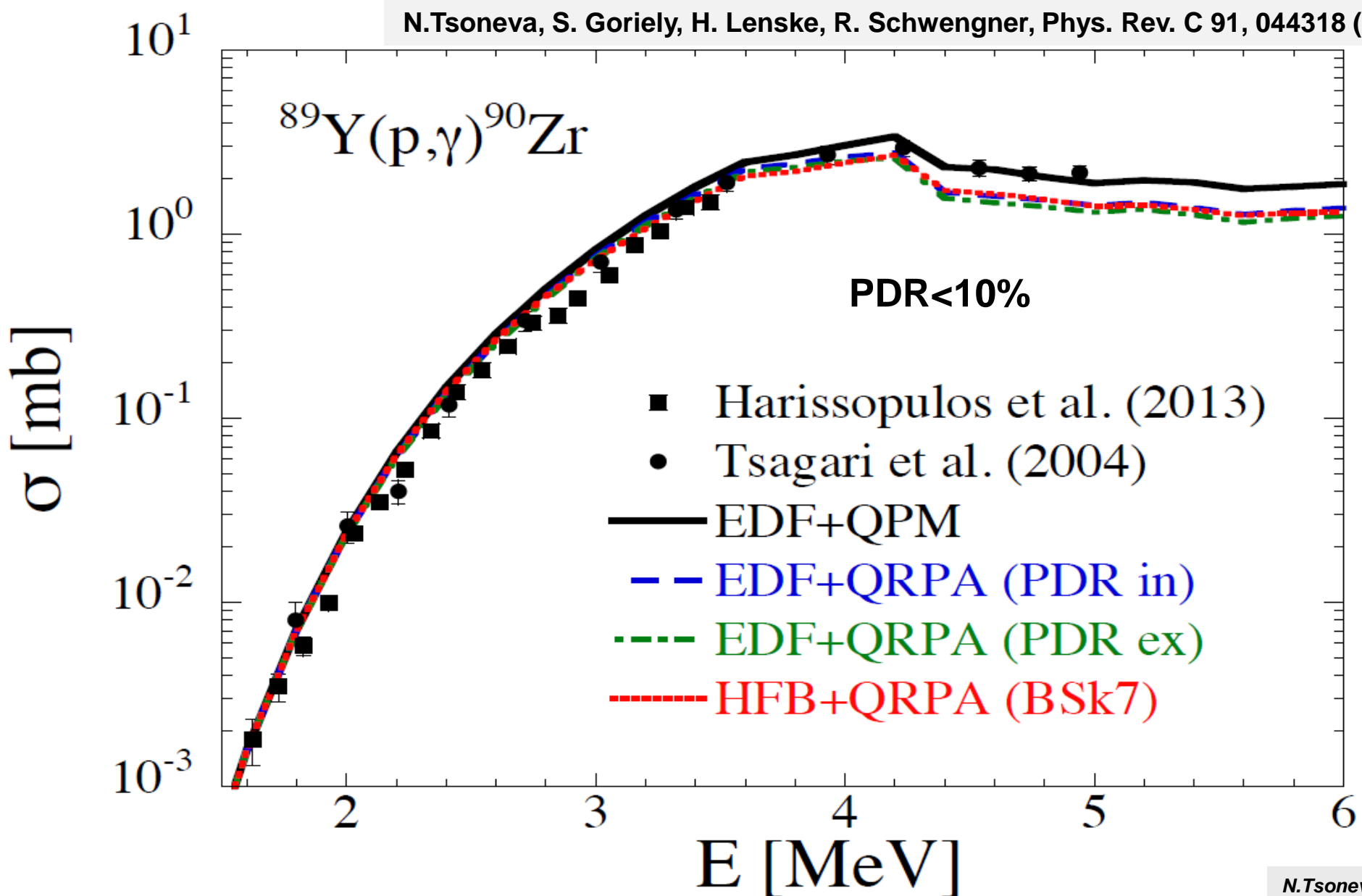
N. Tsoneva, S. Goriely, H. Lenske, R. Schwengner, Phys. Rev. C91, 044318 (2015).



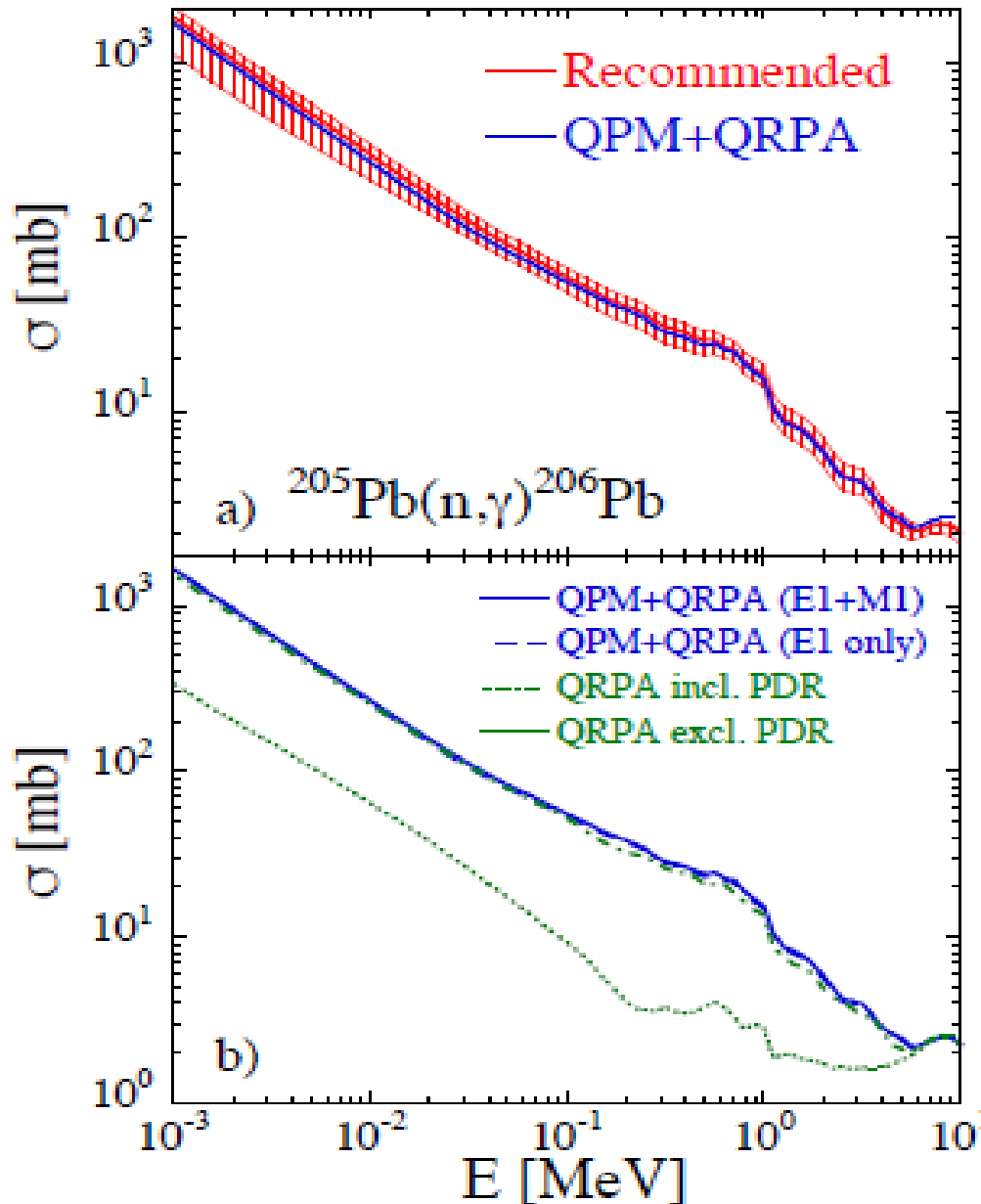
$^{85}\text{Kr}(n,\gamma)^{86}\text{Kr}$  cross sections, the hashed area corresponds to the cross section determined with the experimental strength as derived in R. Raut et al., Phys. Rev. Lett. 111, 112501 (2013).

$^{87}\text{Sr}(n,\gamma)^{88}\text{Sr}$ , TALYS cross sections are compared with experimental data G. Walter, Kernforschungszentrum Karlsruhe Reports No.3706 (1984); R.L. Macklin and J.H. Gibbons, Phys. Rev. 159, 1007 (1967).

# Proton capture cross section of the $^{89}\text{Y}(\text{p},\gamma)^{90}\text{Zr}$ : Calculations with TALYS using EDF+QRPA, HFB+QRPA and three-phonon QPM strength functions



# Nuclear Pygmy Modes as Doorways to Nucleosynthesis: Destruction of the s-process $^{205}\text{Pb}$ nuclide by n-capture via the PDR ?



• At stellar temperature of  $kT = 30 \text{ keV}$   
MACS of  $130(+25,-25) \text{ mb}$

⇒ The combined PDR plus core polarization contribution is crucial !

⇒ M1 contribution small, less than 5%.

# Collection of Observables Probing the n-p Matter

$$\Delta r_{np} = \sqrt{\langle r^2 \rangle_n} - \sqrt{\langle r^2 \rangle_p},$$

## Symmetry Energy

$$S(\rho) \equiv \frac{1}{2} \left( \frac{\partial^2 \mathcal{E}(\rho, \alpha)}{\partial \alpha^2} \right)_{\alpha=0} \approx \mathcal{E}(\rho, \alpha=1) - \mathcal{E}(\rho, \alpha=0)$$

## Density Dependence of the Symmetry Energy

$$S(\rho) = J + Lx + \frac{1}{2}K_{\text{sym}}x^2 + \dots \quad \text{with } x \equiv \frac{\rho - \rho_0}{3\rho_0}.$$

## Nuclear Dipole Polarizability and Photoabsorption

$$\alpha_D = \frac{1}{2\pi^2\alpha} \int_0^\infty \frac{\sigma_\gamma(E)}{E^2} dE = \frac{\sigma_{-2}}{2\pi^2\alpha}$$

# Moments of the photoabsorption cross section

Nucleus	$E_{\max}$ (MeV)	$60NZ/A$ (mb MeV)	$\sigma_0$ (mb MeV)	$\sigma_{-1}$ (mb)	$\sigma_{-2}$ (mb/MeV)	Ref.
$^{206}\text{Pb}$	26.4	2961.6	$3543.7 \pm 293.9$	$241.0 \pm 17.4$	$17.6 \pm 1.4$	Present+[51, 52]
			3436.5	239.8	17.6	[ENDF]
	25.0	2961.6	3060.1	230.4	18.3	EDF+QPM
$^{208}\text{Pb}$	25.0	2980.4	$3980.6 \pm 331.4$	$286.7 \pm 17.8$	$20.4 \pm 1.0$	[53]
			3404	239.3	17.7	[ENDF]

## Photoabsorption cross section and Nuclear Matter

Model	$\sigma_0$ (mb MeV)	$\sigma_{-1}$ (mb)	$\sigma_{-2}$ (mb/MeV)	$R_{\text{skin}}$ (fm)	$J$ (MeV)	$L$ (MeV)	$K_{\text{sym}}$ (MeV)
RMF012	3652.8	237.4	17.4	0.116 [0.128]	29.8	48.3	98.7
FSUGarnet	3688.7	243.4	18.1	0.147 [0.161]	30.9	51.0	59.5
FSUGold	3637.8	251.0	19.4	0.190 [0.207]	32.6	60.5	-51.3
RMF028	3710.6	265.1	21.4	0.263 [0.285]	37.5	112.6	26.2
RMF032	3811.9	262.2	20.8	0.295 [0.320]	41.3	125.6	28.6
GiEDF	3060.1	230.4	18.3	0.151 [0.158]	33.4	53.9	-188.4

# Summary and Outlook

- New low-energy modes: PDR, PQR ...
- GiEDF+QPM: an extended DFT plus multi-phonon approach to nuclear spectra and astrophysics
- Subthreshold pygmy modes, multi-phonon excitations, GDR and capture cross sections
- Correlations: PDR  $\leftrightarrow$  skin thickness  $\leftrightarrow$  polarizability  $\leftrightarrow$  slope L  $\leftrightarrow$  ...?
- Predictions of s- and r-process nucleosynthesis rates

A large, stylized 3D text graphic that says "Thank you!" in a bold, blocky font. The letters are primarily blue with orange highlights, giving them a metallic or glowing appearance.

In collaboration with:

H. Lenske, V. Derya, S. Goriely, J. Piekarewicz,  
R. Schwengner, M. Spieker, A. Tonchev, W. Tornow ...